Acetylcholinesterase-Catalyzed Hydrolysis of Anilides: Acylation Reaction Dynamics and Intrinsic Chemical Transition-State Structures

Paul N. Barlow,† Scott A. Acheson, Michael L. Swanson, and Daniel M. Quinn*

Contribution from the Department of Chemistry, The University of Iowa, Iowa City, Iowa 52242.
Received May 27, 1986

Abstract: The acylation stages of acetylcholinesterase-catalyzed hydrolyses of the anilides *o*-nitrochloroacetanilide (ONCA), *o*-nitroformanilide (ONFA), and *o*-nitroacetanilide (ONA) are rate limited by virtual transition states that are weighted averages of contributions from solvent isotope sensitive and solvent isotope insensitive microscopic transition states. [Quinn, D. M.; Swanson, M. L. *J. Am. Chem. Soc.* **1984**, *106*, 1883-1884. Acheson, S. A.; Barlow, P. N.; Lee, G. C.; Swanson, M. L.; Quinn, D. M. *J. Am. Chem. Soc.*, preceding paper in this issue.] Increasing concentrations of Me_2SO ($\leq$10% (v/v)) competitively inhibit the ONCA reaction and effect a change in rate-determining step for the ONA and ONCA reactions. Experimental observations that support this model include the following: (a) The Eyring plots for V/K are curvilinear downward for both substrates, which is consistent with contributions to rate determination from serial microscopic steps. (b) In the presence of 1.0% Me_2SO (v/v), V/K for ONCA is reduced by 65% at 25 °C, the temperature sensitivity of V/K is increased, and the Eyring plot is linear. Similar results are obtained for ONA in the presence of 5% Me_2SO (v/v). (c) The solvent isotope effect for V/K of ONCA hydrolysis increases from 1.31 ± 0.02 in the absence of Me_2SO to 1.94 ± 0.04 in the presence of 10% Me_2SO (v/v). The solvent isotope effect for ONA hydrolysis changes from 1.55 ± 0.06 to 1.92 ± 0.02 in the presence of 5% Me_2SO (v/v). (d) Proton inventories for V/K of ONCA hydrolysis are linear when the reaction medium contains either 1.0% or 10% Me_2SO (v/v). The ONA proton inventory is linear in the presence of 5% Me_2SO (v/v). These results indicate that inhibition by Me_2SO is accompanied by a shift from a virtual transition state to a prominently rate limiting chemical transition state that is stabilized by a single proton bridge. Therefore, AChE behaves as a simple general acid-base catalyst during the acylation stage of the mechanism. The solvent isotope effects for V/K and V of ONCA hydrolysis, along with the intrinsic solvent isotope effect determined for the corresponding Me_2SO inhibited reaction, allow one to calculate the relative free energies of serial ES complexes that precede the respective acylenzymes. By using these data and relative acylation transition state free energies that are calculated from proton inventories in the absence of Me_2SO (described in the preceding paper in this issue), one can formulate free energy diagrams for the acylation stage of AChE-catalyzed hydrolysis of anilides. The picture which emerges from this analysis is that acylation reaction dynamics involve successive ES complexes of similar free energies which respectively precede transition states of similar free energies.

The transition states for chemical steps of the acylation stage of acetylcholinesterase (AChE[1]) catalysis have until recently proved difficult to characterize. This situation obtains because acylation appears to be rate limited by nonchemical events for all but the least reactive ester substrates.[2-4] Hogg et al.[2] have suggested that conformation changes contribute to acylation rate determination, while Rosenberry[3,4] has implicated induced fit conformation changes that precede chemical catalysis. Quinn and Swanson[5] investigated the acylation transition state for the anilide ONCA by using pH-rate effects and solvent deuterium kinetic isotope effects. ONCA was chosen because it is 10^2-fold less reactive than but is closely isosteric with good phenyl ester substrates.[6] It was hoped that the much lower intrinsic acylation reactivity of ONCA would lead to exposure of chemical transition states. However, analysis of the proton inventory for V/K of AChE-catalyzed hydrolysis of ONCA indicated that the solvent isotope sensitive step is only ~30% rate limiting.[5] Consequently, the observed solvent isotope effect of 1.4 results from a chemical transition state that is stabilized by proton transfer (and which gives an intrinsic solvent isotope effect of ~2) but which is masked by prominent rate determination by a solvent isotope insensitive step.

In this paper we describe additional solvent deuterium kinetic isotope effect investigations of AChE-catalyzed hydrolysis of anilides. Isotope effects for V/K and V, which both monitor acylation, are used to characterize acylation reaction dynamics and transition-state structures. Me_2SO is shown to be a competitive inhibitor of anilide hydrolyses. However, large increases in solvent isotope effects for V/K of ONCA and ONA hydrolyses accompany Me_2SO inhibition, which indicates that chemical transition states have become prominently rate limiting. This fact is exploited herein to characterize proton transfer catalytic stabilization of the chemical step by using the proton inventory technique. Furthermore, an acylation reaction dynamics model is proposed which contains the following features: (a) In the absence of Me_2SO, an isomerization of the initial ES complex (ES_1) dominates rate limitation.[3-5,7] (b) Isomerization produces ES_2, which is more stable than ES_1. (c) Chemical catalysis follows isomerization and involves a transition state that is stabilized by simple general acid-base proton bridging.

Experimental Section

Materials. Protium oxide used for buffer preparation was distilled and deionized by passage through a Barnstead mixed-bed ion-exchange column (Sybron Corp.). Deuterium oxide (>99.9% D) and acetonitrile (spectrophotometric grade) were obtained from Aldrich Chemical Co. and were used as received. Grade V-S AChE (EC 3.1.1.7) from *Electrophorus electricus* was obtained as a lyophilized powder from Sigma Chemical Co. Prior to use the enzyme was dissolved in 0.1 M sodium

† Present address: Department of Biophysics, The University of Chicago, Chicago, Illinois 60637.

* To whom correspondence should be addressed. This work was supported by NIH Grant NS21334. D.M.Q. is the recipient of a NIH Research Career Development Award (HL01583).

(1) Abbreviations: AChE, acetylcholinesterase; ONA, *o*-nitroacetanilide; ONCA, *o*-nitrochloroacetanilide; ONFA, *o*-nitroformanilide; ONPA, *o*-nitrophenyl acetate; V/K, V_{max}/K_m; V, V_{max}; K, K_m; ^{D_2O}V, solvent deuterium kinetic isotope effect for V_{max}; $^{D_2O}V/K$, solvent deuterium kinetic isotope effect for V/K; Me_2SO, dimethyl sulfoxide; E, free enzyme; EA, acylenzyme; ES_1, Michaelis complex; ES_2, induced fit complex; L, H (hydrogen) or D (deuterium); k_{ES}, k_{cat}; k_E, k_{cat}/K_m.

(2) Hogg, J. L.; Elrod, J. P.; Schowen, R. L. *J. Am. Chem. Soc.* **1980**, *102*, 2082-2086.
(3) Rosenberry, T. L. *Proc. Natl. Acad. Sci. U.S.A.* **1975**, *72*, 3834-3838.
(4) Rosenberry, T. L. *Adv. Enzymol. Rel. Areas Mol. Biol.* **1975**, *43*, 103-218.
(5) Quinn, D. M.; Swanson, M. L. *J. Am. Chem. Soc.* **1984**, *106*, 1883-1884.
(6) Naveh, M.; Bernstein, Z.; Segal, D.; Shalitin, Y. *FEBS Lett.* **1981**, *134*, 53-56.
(7) Acheson, S. A.; Barlow, P. N.; Lee, G. C.; Swanson, M. L.; Quinn, D. M. *J. Am. Chem. Soc.*, preceding paper in this issue.

0002-7863/87/1509-0253$01.50/0 © 1987 American Chemical Society

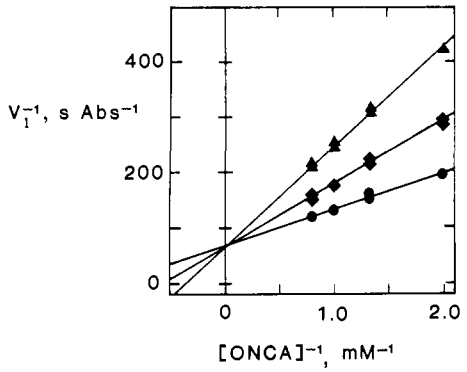

Figure 1. Competitive inhibition of AChE-catalyzed hydrolysis of ONCA by Me_2SO. Reactions were conducted at 25.00 ± 0.05 °C and pH 7.26 in 1.00 mL of 0.1 M sodium phosphate buffer that contained 0.1 N NaCl, 23 nM AChE, the indicated concentrations (as reciprocals) of ONCA, and 0% Me_2SO (●), 0.4% Me_2SO (v/v) (♦), or 1.0% Me_2SO (v/v) (▲).

phosphate buffer, pH 7.30, that contained 0.1 N NaCl. The buffered enzyme was stored at −20 °C and was stable for over a month. Quantitation of AChE active site concentration and synthesis and characterization of the anilide substrates are described by Acheson et al.[7] Me_2SO purchased from Baker Chemical Co. was distilled prior to use.

Enzyme Kinetics and Data Reduction. Timecourses for the hydrolysis of *o*-nitroanilides were followed at 413 nm with Beckman DU7 or DU40 UV-vis spectrophotometers that are interfaced to IBM Personal Computers. Reactions were conducted in 1.00 mL of buffer in quartz cells in the water-jacketted cell holders of the spectrophotometers. Reaction temperature was controlled to ±0.05 °C by using VWR 1140 or Lauda RC3 refrigerated, circulating water baths. The preparation and pL (L = H, D) determination of equivalent buffers in H_2O and D_2O and the preparation of stock substrate solutions are as described by Acheson et al.[7]

Initial velocities were calculated by linear-least-squares analysis of timecourses that comprise ≤5% of total substrate turnover. First-order rate constants (V/K's) were calculated by nonlinear-least-squares fitting of timecourses that comprise over 3 half-lives of substrate turnover, as described in the preceding paper.[7] Nonlinear-least-squares analysis of curvilinear Eyring plots is also described in the preceding paper.

Results

Inhibition by Me_2SO. Me_2SO acts as a competitive inhibitor of AChE-catalyzed hydrolysis of ONCA and ONA. Figure 1 shows the Lineweaver–Burk pattern for Me_2SO inhibition of ONCA hydrolysis, which is consistent with the assigned inhibition mechanism. Competitive inhibition is not simply due to competition between Me_2SO and substrate for binding to the free enzyme, as Figure 2 demonstrates. As Me_2SO inhibition increases, the solvent isotope effects for ONCA and for ONA (data not shown) hydrolyses increase, eventually reaching ~2. These solvent isotope effects are similar in magnitude to the intrinsic solvent isotope effects on k_3 calculated by nonlinear-least-squares analysis of curvilinear proton inventories for ONCA[5] and ONA[7] hydrolyses in the absence of Me_2SO. Hence, Me_2SO inhibition induces a change in rate-determining step that exposes a chemical transition state that is stabilized by proton transfer. The proton inventory experiments described in the next paragraph indicate that the proton transfer transition state has become solely or prominently rate determining. Solvent isotope effects for V and V/K and intrinsic solvent isotope effects for k_3 of AChE-catalyzed anilide hydrolyses are given in Table I.

Proton Inventories. Proton inventories[8-10] for V/K of AChE-catalyzed hydrolysis of ONCA in the presence of 10% Me_2SO (v/v) (Figure 3A) and of ONA in the presence of 5% Me_2SO (v/v) (Figure 3B) are linear. The proton inventory for V/K of ONCA hydrolysis in the presence of 1% Me_2SO (v/v) is also linear

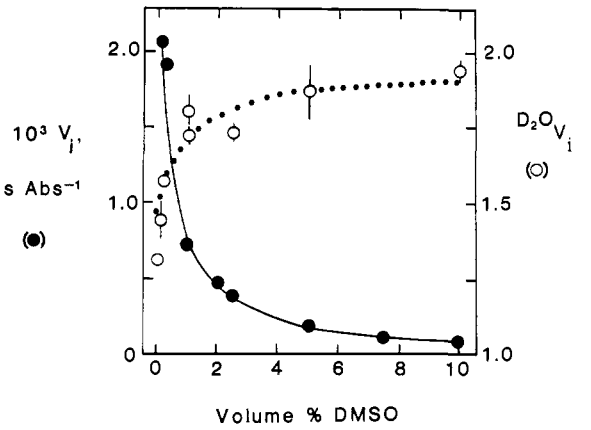

Figure 2. Effect of Me_2SO on the velocity of and solvent isotope effect for AChE-catalyzed hydrolysis of ONCA. Reactions were conducted at 25.00 ± 0.05 °C and pH 7.24 (H_2O) or pD 7.86 (D_2O) in 1.00 mL of 0.1 M sodium phosphate buffer that contained 0.1 N NaCl, 55–317 nM AChE, the indicated concentrations of Me_2SO, and $[ONCA]_0$ = 0.05–0.5 mM. V/K's were determined either by measuring initial velocities at $[ONCA]_0 \ll K_m$, or by nonlinear-least-squares analysis of first-order timecourses. The curved line through the V/K's is a nonlinear-least-squares fit to eq 19 of the Discussion. The dotted line through the $^{D_2O}V/K$'s is a nonlinear-least-squares fit to eq 18 of the Discussion.

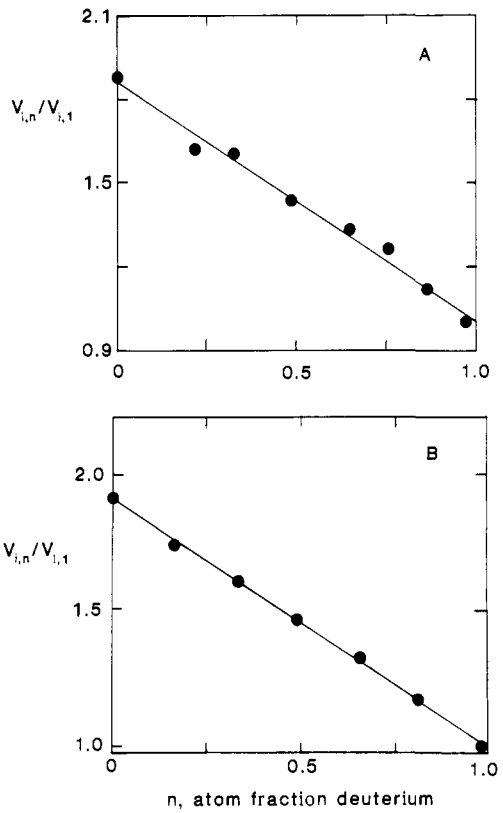

Figure 3. Proton inventories for Me_2SO-inhibited AChE-catalyzed anilide hydrolyses. The data are plotted as partial solvent isotope effects ($V_{i,n}/V_{i,1}$) vs. n. V_i's are initial velocities that were calculated as described in the Experimental Section. (A) Proton inventory for ONCA. Reactions were conducted at 25.00 ± 0.05 °C in 1.00 mL of 0.1 M sodium phosphate buffer, pH 7.26 and equivalent pL,[7-10] that contained 0.1 N NaCl, 10% Me_2SO (v/v), 55 nM AChE, and $[ONCA]_0$ = 1.0 mM ($\ll K_m$). (B) Proton inventory for ONA. Reactions were conducted as described above, save that they contained 5% Me_2SO (v/v), 126 nM AChE, and $[ONA]_0$ = 0.5 mM. K_m for ONA in the absence of Me_2SO is 20 mM.[7]

(plot not shown) and is accompanied by a solvent isotope effect of 1.80 ± 0.05. The linearity of the plots indicates that the proton transfer transition states that are exposed by Me_2SO inhibition are stabilized by simple general acid–base catalysis.[11,12] The

(8) Schowen, K. B. J. In *Transition States of Biochemical Processes*; Gandour, R. D., Schowen, R. L., Eds.; Plenum: New York, 1978; pp 225–283.
(9) Schowen, K. B.; Schowen, R. L. *Methods Enzymol.* **1982**, *87*, 551–606.
(10) Venkatasubban, K. S.; Schowen, R. L. *Crit. Rev. Biochem.* **1984**, *17*, 1–44.

Table I. Solvent Isotope Effects for AChE-Catalyzed Anilide Hydrolyses

solvent isotope effect	substrate		
	ONCA	ONA	ONFA
$^{D_2O}V/K$[a]	1.31 ± 0.02	1.55 ± 0.03	1.41 ± 0.03
^{D_2O}V[b]	1.75 ± 0.03		1.85 ± 0.09
$^{D_2O}k_3$	1.94 ± 0.04[c]	1.92 ± 0.02[d]	2.3 ± 0.3[e]
	2.3 ± 0.2[e]	2.5 ± 0.2[e]	

[a] Solvent isotope effects for V/K are taken from ref 7. [b] Solvent isotope effects for V were calculated from the intercepts of Lineweaver–Burk plots constructed from initial velocities that were measured at 25.00 ± 0.05 °C. Reactions were conducted in 1.00 mL of 0.1 M sodium phosphate buffer, pH 7.30 or pD 7.86, that contained 0.1 N NaCl, 2% CH_3CN (v/v), 23 nM AChE (ONCA reactions), or 65 nM AChE (ONFA reactions) and varying concentrations of substrates. [c] Calculated from a linear-least-squares fit of the ONCA proton inventory for reactions conducted in the presence of 10% Me_2SO (v/v) (see Figure 3A). [d] Calculated from a linear-least-squares fit of the ONA proton inventory for reactions conducted in the presence of 5% Me_2SO (v/v) (see Figure 3B). [e] Taken from ref 7.

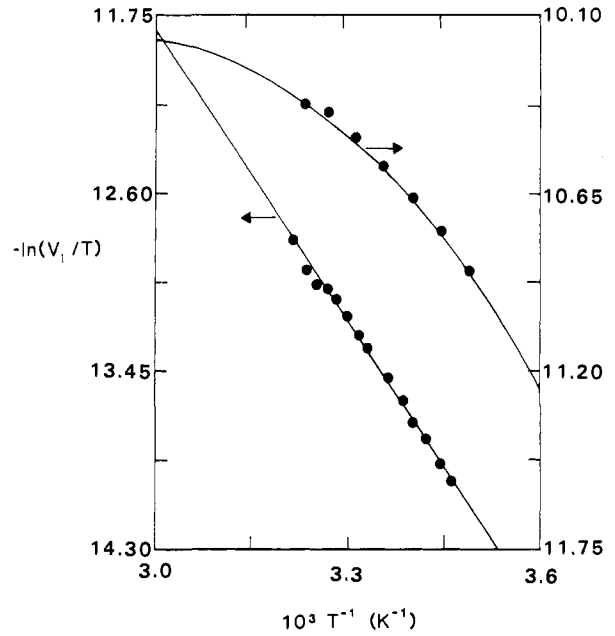

Figure 4. Eyring plots for AChE-catalyzed hydrolysis of ONCA. Reactions were conducted at pH 7.30 and the indicated temperatures (as reciprocals) in 1.00 mL of 0.1 M sodium phosphate buffer that contained 0.1 N NaCl. Upper plot: Rate constants were determined by nonlinear-least-squares analysis of first-order timecourses. Reactions contained 65 nM AChE and $[ONCA]_0 = 0.04$ mM ($=K_m/20$). Lower plot: Rate constants are initial velocities. Reactions contained 1% Me_2SO (v/v), 40 nM AChE, and $[ONCA]_0 = 0.25$ mM ($=K_m/11$).

solvent isotope effects calculated from the displayed linear-least-squares fits of the proton inventories are given in Table I.

Temperature Dependence of ONCA Hydrolysis. Figure 4 shows Eyring plots for V/K of AChE-catalyzed hydrolysis of ONCA. In the absence of Me_2SO the Eyring plot is curvilinear downward, and nonlinear-least-squares analysis (as described in the preceding paper[7]) gives the following enthalpies of activation: $\Delta H^{\ddagger}_2 = 0.0 \pm 0.4$ kcal mol^{-1} and $\Delta H^{\ddagger}_3 = 10.0 \pm 0.5$ kcal mol^{-1}. In the presence of 1% Me_2SO (v/v) the ONCA Eyring plot is linear (or nearly so), and linear-least-squares analysis gives $\Delta H^{\ddagger} = 9.2 \pm 0.1$ kcal mol^{-1}. The similarity between $\Delta H^{\ddagger}_3$ and $\Delta H^{\ddagger}$ suggests that the microscopic step whose temperature dependence is characterized in the presence of 1% Me_2SO is the same step as that with the greater temperature dependence in the absence of Me_2SO. In addition, because Me_2SO inhibition leads to the expression of a solvent isotope effect of ~2, the step with the greater temperature dependence in the absence of Me_2SO must be the solvent isotope sensitive step.

Table II. Reaction Dynamics and Thermodynamics for AChE-Catalyzed Anilide Hydrolyses

parameter	substrate		
	ONCA	ONA	ONFA
k_E,[a] M^{-1} s^{-1}	1.03×10^5	7.8×10^3	1.94×10^3
K_m,[a] mM	0.8 ± 0.1	20 ± 3	2.1 ± 0.2
K_d, mM	0.33 ± 0.05		1.0 ± 0.2
C[b]	2.0 ± 0.2	1.4 ± 0.2	
	2.0 ± 0.5	1.4 ± 0.3	2.0 ± 0.6
R	0.25 ± 0.10		0.5 ± 0.3
k_2/k_{-2}	7.0 ± 3.5		3.0 ± 2.7
k_{-1}/k_1, mM	2.6 ± 1.2		
$\Delta G_E^{\ddagger}$, kcal mol^{-1}	18.8	20.3	21.2
$\Delta G_2^{\ddagger}$, kcal mol^{-1}	18.6	20.0	21.0
$\Delta G_3^{\ddagger}$, kcal mol^{-1}	18.1	19.8	20.5
ΔG_{ES}, kcal mol^{-1}	4.0	5.9	4.5
ΔG_1, kcal mol^{-1}	4.7		4.9
ΔG_2, kcal mol^{-1}	4.2		4.9

[a] K_m's are taken from ref 7, and k_E's are calculated from data in the same reference. [b] The first row of commitments are calculated by using eq 4 and the data of Table I. The intrinsic solvent isotope effects for k_3 used in the calculations are those for the Me_2SO-inhibited ONCA and ONA reactions. The second row of commitments are from ref 7.

Scheme I

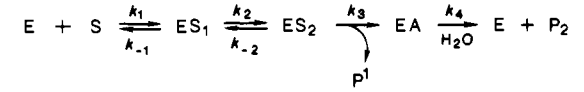

K_m and K_d Determinations for ONFA and ONCA Hydrolyses. Klinman and Matthews[13] have outlined a method for determining an enzyme–substrate dissociation constant from the substrate's K_m and from the reduced solvent isotope effects for V and V/K. Their relationship among these quantities, cast in terms of solvent deuterium kinetic isotope effects for V and V/K, is given in eq 1. K_d in this equation is the dissociation constant of substrate

$$\frac{^{D_2O}V - 1}{^{D_2O}V/K - 1} = K_m/K_d \qquad (1)$$

from all ES complexes that precede the isotopically sensitive step.[13] K_m for ONFA hydrolysis is 2.1 ± 0.2 mM.[7] ^{D_2O}V and $^{D_2O}V/K$ are 1.85 ± 0.09 and 1.41 ± 0.03,[7] respectively. The value for K_d calculated by plugging these values into eq 1 is 1.0 ± 0.2 mM. These results and those of similar calculations for ONCA are given in Table II.

Discussion

The data presented in this paper present a rare opportunity to construct a thorough accounting of reaction dynamics and chemical transition-state structures for AChE catalysis. For the anilides ONCA, ONA, and ONFA, V monitors rate-determining acylation. The k_{cat}'s of acyl-similar anilide and ester substrates support this assignment. For example, k_{cat}'s for *p*-methoxyphenyl formate and ONFA[7] are 6.26×10^3 s^{-1} and 4.1 s^{-1}, respectively. Those for phenyl chloroacetate[12] and ONCA are 366 and 82 s^{-1}, respectively; those for phenyl acetate[12] and ONA are 2.72×10^3 and 156 s^{-1}, respectively. Were deacylation rate limiting for anilide substrates at substrate saturation, k_{cat}'s for the constituents of each acyl-similar pair of substrates would be the same.

The mechanism for AChE catalysis proposed by Rosenberry[4] and utilized by Acheson et al.[7] reduces to that of Scheme I when pH $\gg$ pK_a. During the acylation stage of catalysis a kinetically significant isomerization of ES_1 to ES_2 (induced fit[3,4,7]) precedes chemical catalysis, k_3. As before,[5,7] we assume that only k_3 is subject to an appreciable solvent isotope effect. For the rate-

(11) Kovach, I. M.; Larson, M.; Schowen, R. L. *J. Am. Chem. Soc.* **1986**, *108*, 3054–3056.
(12) Acheson, S. A.; Dedopoulou, D.; Quinn, D. M. *J. Am. Chem. Soc.* **1986**, penultimately preceding paper in this issue.
(13) Klinman, J. P.; Matthews, R. G. *J. Am. Chem. Soc.* **1985**, *107*, 1058–1060.

determining acylation discussed above, the mechanism of Scheme I yields eq 2 and 3 for the phenomenological kinetic parameters.

$$k_E = \frac{k_1k_2k_3}{k_{-1}(k_{-2} + k_3)} \quad (2)$$

$$k_{ES} = \frac{k_2k_3}{k_{-2} + k_2 + k_3} \quad (3)$$

In these equations, $k_E = k_{cat}/K_m$ and $k_{ES} = k_{cat}$. The solvent isotope effects for V/K and for V are given by eq 4 and 5, respectively.

$$^{D_2O}V/K \equiv k_E^{H_2O}/k_E^{D_2O} = \frac{^{D_2O}k_3 + C}{1 + C}, \text{ where } C = k_3/k_{-2} \quad (4)$$

$$^{D_2O}V \equiv k_{ES}^{H_2O}/k_{ES}^{D_2O} = \frac{^{D_2O}k_3 + R}{1 + R}, \text{ where } R = \frac{C}{1 + k_2/k_{-2}} \quad (5)$$

Equation 6 is derived from eq 4 and 5:

$$\frac{^{D_2O}V - 1}{^{D_2O}V/K - 1} = \frac{1 + C}{1 + R} \quad (6)$$

Hence, if the solvent isotope effects for V and V/K are known and the commitment to proton transfer catalysis (C)[5,7,12] can be determined, one can calculate k_2/k_{-2}. Commitments and values of k_2/k_{-2} for the AChE-catalyzed hydrolyses of ONA, ONFA, and ONCA are given in Table II. For ONCA and ONA commitments were calculated by using eq 4 and the solvent isotope effects for V/K in Table I. The intrinsic solvent isotope effects for k_3 (i.e., $^{D_2O}k_3$) used to calculate commitments are those in Table I for the respective Me_2SO-inhibited reactions. The calculated commitments are in good agreement with those determined by Acheson et al.[7] by least-squares analysis of nonlinear proton inventories for AChE-catalyzed anilide hydrolyses. Furthermore, the solvent isotope effects of Table I can be used to calculate the substrate dissociation constant K_d by using eq 1, as outlined by Klinman and Matthews.[13] Since $K_d^{-1} = K_1^{-1} + K_2^{-1}$, where $K_1 = k_{-1}/k_1$ and $K_2 = k_{-1}k_{-2}/k_1k_2$, one can also calculate k_{-1}/k_1, the dissociation constant of ES_1. These values are given in Table II.

The values for C and k_2/k_{-2} can be used to construct a quantitative free energy diagram for AChE-catalyzed anilide hydrolysis. The diagram for the ONCA reaction is elaborated below; those for ONA and ONFA are similar since C's are similar for the various substrates. First we need the free energy of activation for ONCA hydrolysis, which is calculated by using a transform of the Eyring absolute rate theory equation[14] (eq 7), and the free energy for ES complex formation, which is calculated by using eq 8. In eq 7 and 8 k_B, h, R, and T are Boltzmann's constant,

$$\Delta G^{\ddagger}_E = -RT \ln (k_Eh/k_BT) \quad (7)$$

$$\Delta G_{ES} = RT \ln K_m \quad (8)$$

Planck's constant, the gas constant, and the absolute temperature, respectively. Standard states used in the calculation of free energy changes are 10^{-6} M for substrate and 10^{-9} M for E and for ES complexes, including transition states. The substrate standard state was chosen such that the effective reactant state is free enzyme and free substrate, which is the case experimentally when k_E is measured. For ONCA[7] K_m is 8×10^{-4} M and k_E is 1.03×10^5 M^{-1} s^{-1}. Hence, the free energy changes at 25 °C for the acylation stage of AChE-catalyzed hydrolysis of ONCA are $\Delta G^{\ddagger}_E$ = 18.8 kcal mol^{-1} and ΔG_{ES} 4.0 kcal mol^{-1}. However, $\Delta G^{\ddagger}_E$ is not that for conversion of free E and free S to a single transition state because acylation is rate limited by a virtual transition state that contains contributions from the k_2 and k_3 steps.[5,7] Similarly, ΔG_{ES} in the free energy change for conversion of E + S to a virtual, weighted average state that contains contributions from ES_1 and ES_2.

(14) Glasstone, S.; Laidler, K. J.; Eyring, H. *The Theory of Rate Processes*; McGraw-Hill: New York, 1941.

In order to partition $\Delta G^{\ddagger}_E$ into its components for the k_2 and k_3 microscopic steps, eq 2 must be cast in double reciprocal form:

$$k_E^{-1} = k_2'^{-1} + k_3'^{-1} \quad (9)$$

In eq 9 $k_2' = k_1k_2/k_{-1}$ and $k_3' = k_1k_2k_3/k_{-1}k_{-2}$ are the overall rate constants for conversion of the free E and free S reactant state to the transition states of the k_2 and k_3 steps, respectively. By using the Eyring absolute rate theory equation,[14] one can rewrite eq 9 in its equivalent free energy form:

$$e^{\Delta G^{\ddagger}_E/RT} = e^{\Delta G^{\ddagger}_2/RT} + e^{\Delta G^{\ddagger}_3/RT} \quad (10)$$

Furthermore, since $C = k_3/k_{-2}$ and the k_{-2} transition state is also that for k_2:

$$RT \ln C = \Delta G^{\ddagger}_2 - \Delta G^{\ddagger}_3 \quad (11)$$

Equations 10 and 11 are used to solve for the individual free energies of activation in terms of measurable quantities.

$$\Delta G^{\ddagger}_2 = \Delta G^{\ddagger}_E + RT \ln \frac{C}{C+1} \quad (12)$$

$$\Delta G^{\ddagger}_3 = \Delta G^{\ddagger}_E + RT \ln \frac{1}{C+1} \quad (13)$$

In these equations $1/(C + 1) = k_{-2}/(k_{-2} + k_3)$ and $C/(C + 1) = k_3/(k_{-2} + k_3)$ are the fractions of rate limitation of V/K by the k_3 and k_2 steps, respectively. Hence, the microscopic free energies of activation differ from the phenomenological free energy of activation ($\Delta G^{\ddagger}_E$) by quantities that reflect the molecular reaction dynamics for acylation.

A similar approach is used to deconvolute the phenomenological free energy for stable state formation, ΔG_{ES}, into the ΔG components due to ES_1 and ES_2. To do so, we start with the expression for K_m^{-1} for the Scheme I mechanism.

$$K_m^{-1} = K_1^{-1} + [K_2(1 + C)]^{-1} \quad (14)$$

K_1 and $K_2(1 + C)$ are the Michaelis constants for ES_1 and ES_2, respectively. K_1 and K_2 were defined in the text that follows eq 6. With modest rearranging eq 14 becomes:

$$K_m^{-1} = K_1^{-1}\left(1 + \frac{k_2/k_{-2}}{1 + C}\right) \quad (15)$$

Since $\Delta G_1 = RT \ln K_1$ and $\Delta G_2 = RT \ln \{K_2(1 + C)\}$, one can use eq 8 and 15 to construct an expression from which G_1 is calculated.

$$\Delta G_1 = \Delta G_{ES} + RT \ln \left(1 + \frac{k_2/k_{-2}}{1+ C}\right) \quad (16)$$

Finally, since the Michaelis constant for ES_2 is $K_1(k_{-2}/k_2)(1 + C)$, one can derive an expression from which ΔG_2 is calculated.

$$\Delta G_2 = \Delta G_1 + RT \ln \frac{k_{-2}}{k_2}(1 + C) \quad (17)$$

Table II lists the various free energy changes associated with AChE-catalyzed anilide hydrolyses which are calculated by using eq 12, 13, 16, and 17.

Figure 5 is a state-to-state free energy diagram for AChE-catalyzed hydrolysis of ONCA. Several features of this free energy diagram are noteworthy: (a) The profile for stable states runs energetically downhill from ES_1 to the acylenzyme EA. This is so because the anilide hydrolyses are insensitive to product inhibition by *o*-nitroaniline.[15] However, the quantitative difference in free energy between EA and ES_1 or ES_2 is not known, and therefore nothing more is indicated than that the course from ES_1 to EA is exergonic. (b) The binding rate constant k_1 has not been measured, and therefore the free energy for the corresponding transition state is not specified. The k_1 transition state is represented as lower in free energy than consequent acylation tran-

(15) Acheson, S. A.; Quinn, D. M., unpublished observations.

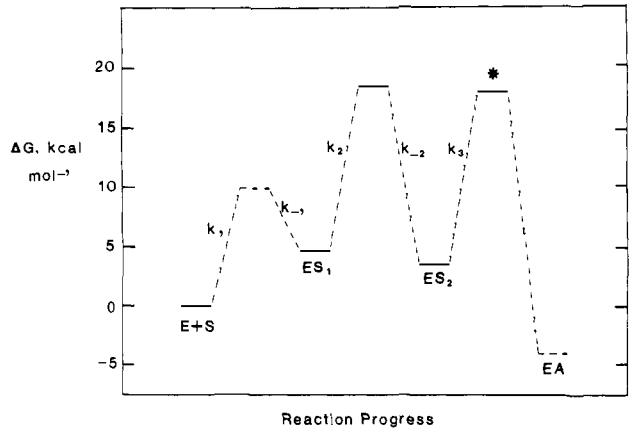

Figure 5. Free energy diagram for AChE-catalyzed hydrolysis of ONCA. States whose free energies are known are denoted by solid lines. Rate and equilibrium constants are described in the text. The solvent isotope sensitive transition state is denoted by an asterisk.

sition states, however. This is equivalent to assuming that binding is rapid and hence kinetically insignificant for V/K. This assumption is reasonable because closely isosteric ester substrates have k_E's that are one to four orders of magnitude greater than those of acyl-similar anilides.[7,12] Since the binding rate constants for structurally similar esters and anilides ought to be similar, binding might be kinetically significant for esters but cannot be so for anilides. (c) Since acylation is rate determining at substrate saturation for anilides, the free energy diagram stops at EA.

Despite the considerations of the preceding paragraph, the ONCA free energy diagram renders a complete accounting of kinetically significant stable states and transition states. Induced fit isomerization of ES_1 produces the more stable ES_2, which immediately precedes the chemical transition state.[16] The chemical transition state is stabilized by, among other factors, one-proton catalysis by AChE. That this is so is supported by the linear proton inventories of Figure 3 for Me_2SO-inhibited ONCA and ONA hydrolyses. Because the stable states and transition states of the free energy profile ramp downhill in parallel, the acylation stage of AChE anilide hydrolyses displays matched internal thermodynamics, which Albery and Knowles[17] say is a feature of reaction dynamics of enzymes that are at or near evolutionary perfection. The Albery and Knowles model has been generalized by Benner[18] to enzyme reactions that are energetically uphill or downhill. The data of Table II show that all three anilides have similar trends in reaction free energetics, and therefore all three reactions display matched internal thermodynamics. Moreover, various aryl ester substrates of AChE have reaction dynamics that are consistent with matched internal thermodynamics,[12] and Rosenberry[3,4] has suggested that various ester substrates and uncharged active site-directed inhibitors react with the enzyme via kinetically significant induced fit. It is interesting that AChE shows this reaction dynamics pattern for substrates that are structurally and functionally remote from the physiological substrate acetylcholine. Perhaps ancestral AChE was a broad-spectrum hydrolytic enzyme and that AChE came upon its physiological function, destruction of the neurotransmitter acetylcholine, relatively recently in evolution. Perhaps not only enzyme catalytic power but also substrate systems evolve to develop the physiological functions necessary to survive.

The free energy diagram of Figure 5 also helps one rationalize why Me_2SO inhibition of AChE-catalyzed anilide hydrolysis is competitive but is accompanied by a change in rate-determining step. If the effect of Me_2SO is to destabilize ES_2 and the k_3 transition state by comparable extents, the K_m will rise, the k_3 transition state will be exposed as rate limiting, the intrinsic solvent isotope effect for k_3 will be unmasked, and the Eyring plot will become linear. These are just the Me_2SO-induced changes that are documented herein. One can quantitatively account for the dependence of $^{D_2O}V/K$ on $[Me_2SO]$ shown in Figure 2 by using this model. Comparable destabilization of ES_2 and the k_3 transition state by Me_2SO means that the commitment to proton transfer catalysis decreases as $[Me_2SO]$ increases. Assume that the commitment decreases as $C/(1 + [I]/K_I)$, where I is Me_2SO. If one substitutes the Me_2SO-dependent commitment into eq 4, eq 18 results.

$$^{D_2O}V/K = \frac{^{D_2O}k_3 + C/(1 + [I]/K_I)}{1 + C/(1 + [I]/K_I)} \qquad (18)$$

In Figure 2, V/K vs. [I] data were fit to eq 19 by nonlinear least squares.

$$(V/K)_I = V/\{K(1 + [I]/K_I)\} \qquad (19)$$

In eq 19 $(V/K)_I$ is V/K in the presence of Me_2SO of concentration [I] and K_I is the dissociation constant of the enzyme–inhibitor complex. The fit gives $K_I = 0.38 \pm 0.08\%$ Me_2SO (v/v) (=0.05 M). This value of K_I was used to perform a nonlinear-least-squares fit of solvent isotope effect data to eq 18 above. The fit, which is represented by the dotted line of Figure 2, yields $^{D_2O}k_3 = 1.95 \pm 0.05$ and $C = 1.1 \pm 0.3$. The commitment is somewhat different than the values in Table II. However, the broad picture which emerges from all determinations of C is the same; i.e., the k_2 and k_3 transition states make comparable contributions to rate determination. Moreover, the calculated intrinsic solvent isotope effect for k_3 is similar to values determined from other experiments. These considerations, along with the fact that the nonlinear fit renders a satisfying account of the dependence of $^{D_2O}V/K$ on [I], indicate that the postulated model for the effects of Me_2SO on AChE-catalyzed hydrolysis of ONCA is probably correct. Corresponding least-squares analyses of Me_2SO effects on V/K and $^{D_2O}V/K$ for AChE-catalyzed hydrolysis of ONA give results that are similar to those displayed in Figure 2 for ONCA.

The detailed characterization of AChE reaction dynamics and transition state structure forwarded in this and in the preceding two papers[7,12] provides a powerful avenue for study of enzyme structure-function. For example, one can ask how changes in such activity modifying factors as metal ion binding or ligand binding[4] affect AChE reaction dynamics. Or one can probe how amino acid modifications or replacements affect molecular reaction dynamics. The number of questions to be addressed is only limited by one's curiosity, imagination, and resources.

(16) It should be noted that the k_3 step might itself be a composite process which consists of serial chemical events, such as formation and breakdown of a tetrahedral intermediate.

(17) Albery, W. J.; Knowles, J. R. *Biochemistry* **1976**, *15*, 5631–5640.
(18) Stackhouse, J.; Nambiar, K. P.; Burbaum, J. J.; Stauffer, D. M.; Benner, S. A. *J. Am. Chem. Soc.* **1985**, *107*, 2757–2763.